Alumina: Discriminative Analysis using 3D Correlation of Solid-State NMR Parameters

C. Vinod Chandran, Christine Kirschhock, Sambhu Radhakrishnan, Francis Taulelle, Johan A. Martens, Eric Breynaert

Center for Surface Chemistry and Catalysis, Celestijnenlaan 200 F, KU Leuven, 3001 Heverlee, Belgium

Chem. Soc. Rev. (2018) DOI: 10.1039/c8cs00321a

1. List of chemical formulae

Table S1. List of chemical formulae

Name	Chemical formula	Popular formula
Gibbsite	$Al(OH)_3$	γ-$Al(OH)_3$
Bayerite	$Al(OH)_3$	α-$Al(OH)_3$
Boehmite	AlO(OH)	γ-AlOOH
Diaspore	AlO(OH)	α-AlOOH
Nordstrandite	$Al(OH)_3$	
Doyleite	$Al(OH)_3$	
Pseudoboehmite	AlO(OH)	
Tohdite (Akdalaite)	$(Al_2O_3)_5.H_2O$	
Alpha-alumina	Al_2O_3	α-Al_2O_3

2. 2D projections of the 3D ellipsoid correlation figures in the main article

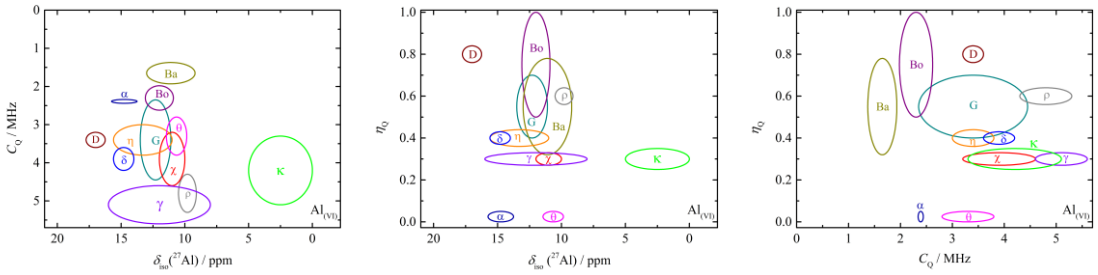

Figure S1: 2D elliptical representations of ^{27}Al NMR parameters (isotropic chemical shift (δ_{iso}), quadrupole coupling constant (C_Q) and asymmetry parameter (η_Q)) for Al(VI) of transition alumina phases (α, χ, κ, θ, γ, δ, η, ρ) and their precursors (Bayerite (Ba), Boehmite (Bo) and Gibbsite (G) and Diaspore (D)). A 3D interactive version of these graphs is available at https://doi.org/10.7910/DVN/FRZEGB. 'Breynaert, C.V. Chandran, 2018, "3D Correlation of Solid-State NMR Parameters for Alumina - 3D interactive chart", https://doi.org/10.7910/DVN/FRZEGB, Harvard Dataverse, V1"'

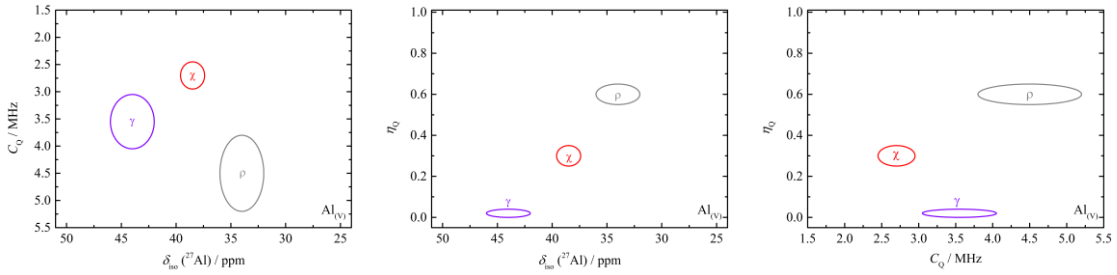

Figure S2: 2D elliptical representations of ^{27}Al NMR parameters (isotropic chemical shift (δ_{iso}), quadrupole coupling constant (C_Q) and asymmetry parameter (η_Q)) for Al(V) of transition alumina phases (χ, γ, ρ). A 3D interactive version of these graphs is available at https://doi.org/10.7910/DVN/FRZEGB. 'Breynaert, C.V. Chandran, 2018, "3D Correlation of Solid-State NMR Parameters for Alumina - 3D interactive chart", https://doi.org/10.7910/DVN/FRZEGB, Harvard Dataverse, V1"'

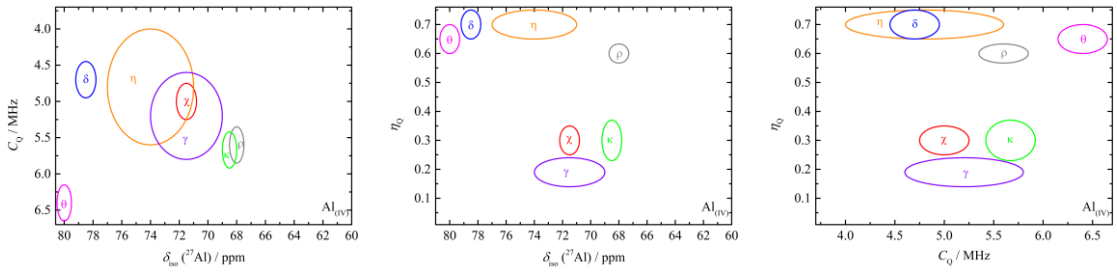

Figure S3: 2D elliptical representations of ^{27}Al NMR parameters (isotropic chemical shift (δ_{iso}), quadrupole coupling constant (C_Q) and asymmetry parameter (η_Q)) for Al(IV) of transition alumina phases (χ, κ, θ, γ, δ, η, ρ). A 3D interactive version of these graphs is available at https://doi.org/10.7910/DVN/FRZEGB. 'Breynaert, C.V. Chandran, 2018, "3D Correlation of Solid-State NMR Parameters for Alumina - 3D interactive chart", https://doi.org/10.7910/DVN/FRZEGB, Harvard Dataverse, V1"'

3. 3D correlation of NMR parameters with the special case of κ-alumina

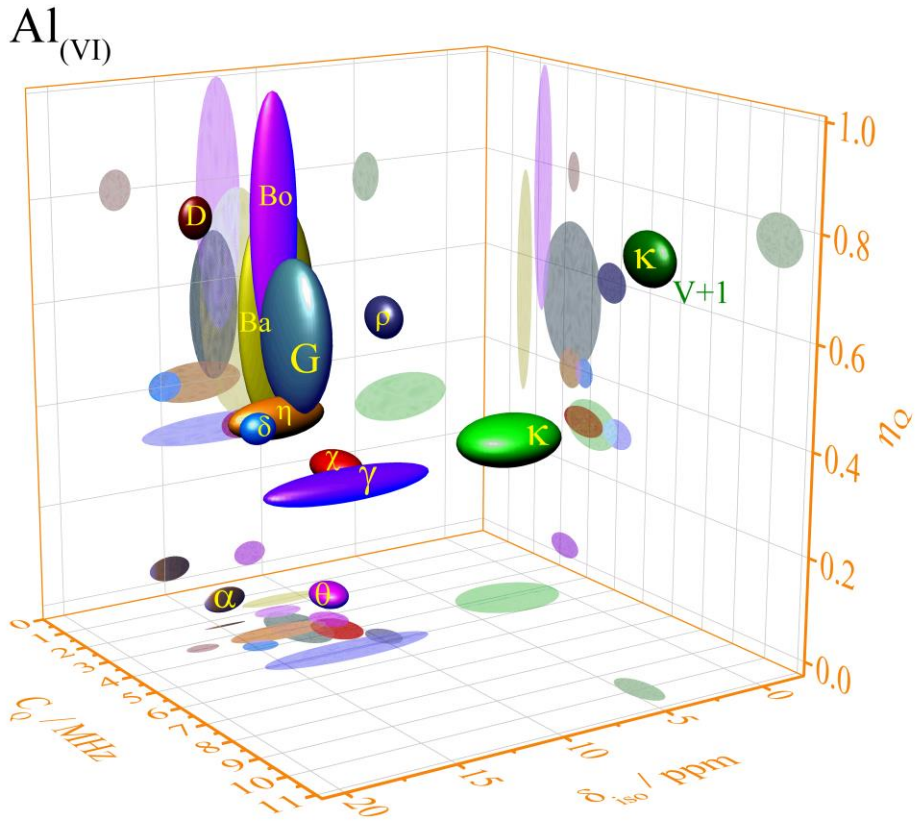

Figure S4. Plots of ^{27}Al NMR parameters (isotropic chemical shift, quadrupole coupling constant and asymmetry parameter) of hexa- Al-O coordinations in transition alumina phases (α, χ, κ, θ, γ, δ, η, ρ) and their precursors (Bayerite (Ba), Boehmite (Bo) and Gibbsite (G) and Diaspore (D)). The phase κ has an additional highly distorted V+1-coordinated site with a high quadrupole coupling of around 10 MHz. A 3D interactive version of this graph is available at https://doi.org/10.7910/DVN/FRZEGB. 'Breynaert, C.V. Chandran, 2018, "3D Correlation of Solid-State NMR Parameters for Alumina - 3D interactive chart", https://doi.org/10.7910/DVN/FRZEGB, Harvard Dataverse, V1'"

4. X-ray Crystallography

Discussion S1: All transition alumina phases are based on a dense packing of oxygen ions and only vary in type of packing (i.e. cubic or hexagonal) and in decoration of the tetrahedral and octahedral voids of the oxygen lattice. This implies all transition alumina systems are symmetrically closely related and therefore also show similar, if not identical, reflections in diffraction. This is especially clear from comparison of structure and diffraction patterns of Gamma and Eta alumina, which both are suggested to be of defective Spinel type and which only differ in the defect sites which predominantly are found on tetrahedral sites for Gamma and on octahedral sites in Eta (blue and red curves in figure S5). The quantification of tetrahedral and hexagonal aluminium in a sample, which could be either of Gamma and Eta type not only is necessary to identify the material but also of utmost importance for determination of the catalytic activity, as Al in tetrahedral coordination has higher acidity compared to Al in octahedral environment.

Provided the sample at hand is highly crystalline, without defects and of large particle size with at least 100nm sized coherently scattering domains, a quantification by diffraction is theoretically possible. The sample would need to be measured on a high resolution diffractometer, and a Rietveld refinement then should allow reasonable quantification of the Al distribution.

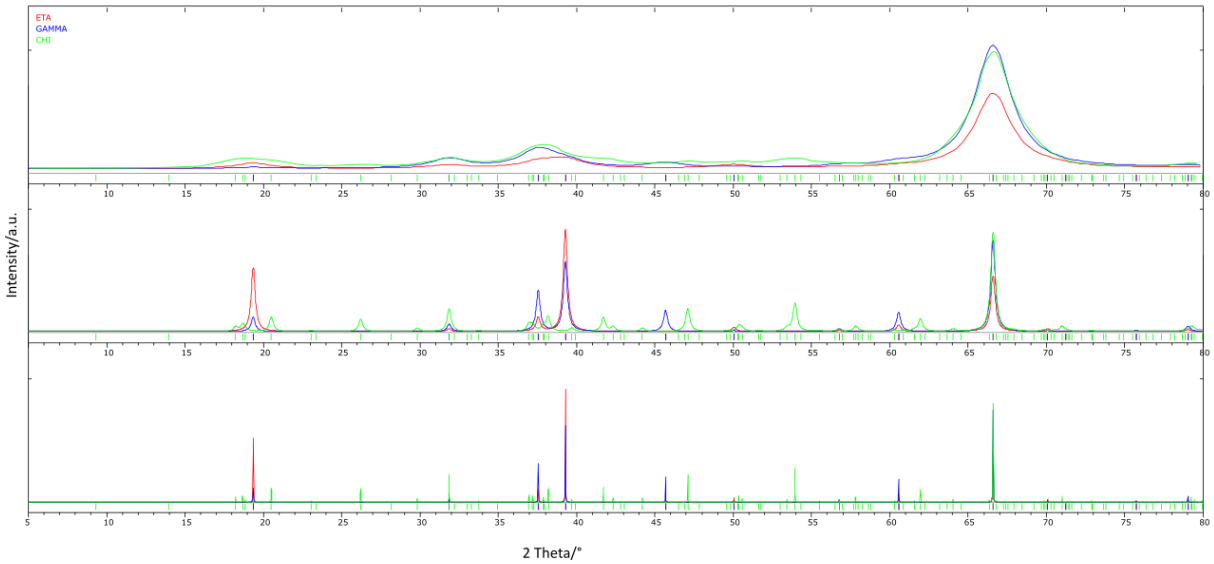

Figure S5. XRD patterns of eta (red), gamma (blue) and chi (green) alumina with particle sizes of 1000 nm (bottom), 100nm (middle) and 10nm (top).

However, the transition alumina phases are derived from layered precursors upon dehydration. This results in increasing degrees of densification, particle fracture, excessive stacking disorder and very often the formation of submicron crystallites. In figure S5 the effect of particle size is shown. Powder patterns simulated for the suggested crystal structures of Gamma, Eta and Chi alumina for different particle sizes. From bottom to top the particle size was 1000nm, 100nm and 10nm. The simulation did not account for commonly encountered stacking disorder, which leads to streaking and further broadening of diffraction lines, nor did it include an amorphous background, which further impedes identification of the intensities of individual reflections. Especially the early transition alumina phases are almost indistinguishable based on their measured powder patterns, which in reality most closely resemble the simulation for app. 10 nm size, and a quantification of their Al distribution is virtually impossible. Even to distinguish Chi from Gamma or Eta in real samples is difficult, even though the first is based on a hcp oxygen lattice while the latter two are cubic.

With increasing degree of dehydration ordering of Al increases and also crystallinity has been observed to improve. However, even so a full structural description of the sample is still out of reach. This most clearly is illustrated by the various structural models still today existing for the Delta phases (red and green traces in Figure S6), which both may simultaneously exist in the same sample.

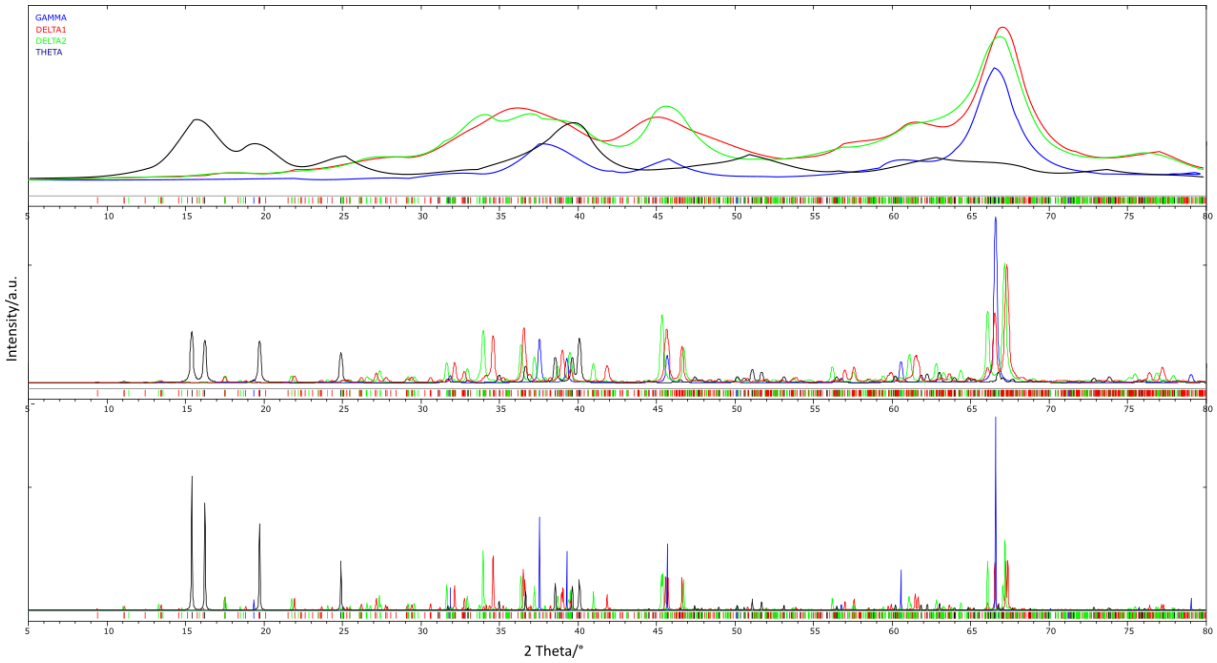

Figure S6. XRD patterns of gamma (blue), delta1 (red), delta2 (green), theta (black) alumina with particle sizes of 1000 nm (bottom), 100nm (middle) and 10nm (top).

Nonetheless, in fortunate cases, where the samples are showing good crystallinity a rough fingerprinting based on the diffraction intensities may be possible, and especially for theta and also kappa quite highly resolved X-ray patterns are known. Even so, the presence of an amorphous background and also incomplete transformation leading to disorder and presence of more than one phase still are preventing a thorough structural analysis based on diffraction only.

5. Czjzek distribution of EFG in alumina phases

Discussion S2: The EFG tensor distribution has been under investigation in the past decade considering its importance in solid-state NMR. Massiot and co-workers [1] introduced the applications of the Czjzek model [2,3] in NMR, which is also known as the Gaussian isotropic model (GIM). This was implemented in the NMR analysis software DMFIT [4] to enable modelling of MAS NMR spectra of quadrupolar nuclei in disordered solids. This model has been widely used to study of amorphous systems containing different isotopes like ^{27}Al [1,5,6] and ^{71}Ga [7–10]. As quadrupolar nuclei in an disordered systems have also distributions in the isotropic chemical shift, this model is equipped with ways to separate the two contributions which cause broadening. However, the model is unable to provide structural information from the distribution analysis [11]. Later an extended version of Czjzek model, [3,11,12] was introduced which claims to be a simple way to generalize the GIM. This improvement takes the EFG of an ordered system into consideration modified by distant perturbations. The local contribution and the distributed Czjzek contribution are taken care of in this method. The relative weight of the local contribution can then be correlated to some structural effects. For a certain EFG tensor obtained from ab initio calculations, this correlation is easily done [1]. Therefore, combined with the calculations the extended model provides useful structural information.
The Czjzek model implemented in DMFIT [13] provides a η_Q of 0.61 for all disordered solids. The values of η_Q reported in the past decades, however vary between 0 and 1, for distributions in EFG, as we see in the case of some of the transition alumina phases. This review has used those reported η_Q values for tabulation. Therefore, we would like to warn the readers who use DMFIT for their data analysis that only one value for η_Q is possible when there is a distribution of the EFG tensor (for phases gamma, eta, chi, rho and delta). For those phases, mainly the correlation between isotropic chemical shift and quadrupole coupling constant should be followed for phase identification. In addition, also the DFT calculations have always resulted in different values for η_Q, starting from ordered structures of many of these alumina phases. Among the different alumina phases only rho-alumina may be considered as a completely amorphous system. All the other phases have different degrees of order. For this reason, the alumina phases cannot be compared with glasses. Therefore, a more legitimate magnitude of η_Q can only be determined in combination with DFT calculations and NMR analysis in the alumina cases with EFG distribution.

Indeed for distributed material assignment of sites and therefore the phase type relies on the set of average values, number of sites, their populations, chemical shifts, quadrupole couplings, and η_Q values. If the same phase is described by different modellings, they may reach average values close enough in DFT calculations, otherwise the modellings are not consistent. The spread depends on the distribution of sites in the material. In case of a distributed material, NMR parameters can be estimated following different types of distribution. When no specific choice appears more justified than another, care has to be taken that the different sets obtained are close enough to be considered equivalent, or else one argument must justify the choice of one model as the best out of the set.

[1] d'Espinose de Lacaillerie J B, Fretigny C and Massiot D 2008 MAS NMR spectra of quadrupolar nuclei in disordered solids: the Czjzek model J. Magn. Reson. 192 244–51

[2] Czjzek G, Fink J, G¨otz F, Schmidt H, Coey J M D, Rebouillat J-P and Li´enard A 1981 Atomic coordination and the distribution of electric field gradients in amorphous solids Phys. Rev. B 23 2513–30

[3] Le Ca¨er G and Brand R A 1998 General models for the distributions of electric field gradients in disordered solids J. Phys.: Condens. Matter 10 10715–74

[4] http://nmr.cemhti.cnrs-orleans.fr/dmfit/default.aspx

[5] Neuville D R, Cormier L and Massiot D 2004 Al environment in tectosilicate and peraluminous glasses: a 27Al MQ-MAS NMR, Raman, and XANES investigation Geochim. Cosmochim. Acta 68 5071–9

[6] Sabarinathan V, Ramasamy S and Ganapathy S 2010 Perturbations to 27Al electric field gradients in nanocrystalline-Al2O3 studied by high-resolution solid-state NMR J. Phys. Chem. B 114 1775–81

[7] Bureau B, Silly G, Buzar´e J Y, Legein C and Massiot D 1999 From crystalline to glassy gallium fluoride materials: an NMR study of 69Ga and 71Ga quadrupolar nuclei Solid State Nucl. Magn. Reson. 14 181–90

[8] Bureau B, Silly G, Buzar´e J Y, Boulard B and Legein C 2000 Nuclear magnetic resonance quadrupolar parameters and short range order in disordered ionic fluorides J. Phys.: Condens. Matter 12 5775

[9] Knijn P J et al 2010 A solid-state NMR and DFT study of compositional modulations in AlxGa1??xAs Phys. Chem. Chem. Phys. 12 11517–35

[10] Mellier C, Fayon F, Schnitzler V, Deniard P, Allix M, Quillard S, Massiot D, Bouler J-M, Bujoli B and Janvier P 2011 Characterization and properties of novel gallium-doped calcium phosphate ceramics Inorg. Chem. 50 8252–60

[11] Le Ca¨er G, Bureau B and Massiot D 2010 An extension of the Czjzek model for the distributions of electric field gradients in disordered solids and an application to NMR spectra of 71Ga in chalcogenide glasses J. Phys.: Condens. Matter 22 065402

[12] Le Ca¨er G, Brand R A and Dehghan K 1985 Sign determination of the 57Fe electric field gradient in amorphous Al70Si17Fe13 J. Physique Coll. 46 C8–169

[13] D. Massiot, F. Fayon, M. Capron, I. King, S. Le Calvé, B. Alonso, JO. Durand, B. Bujoli, Z. Gan, G. Hoaston, Magn. Reson. Chem., 40 (1), 70-76 (2002)